

Theory of pump/probe ARPES in  
1T-TaS<sub>2</sub> via dynamical mean-field  
theory in an effective single-band  
Hubbard model

J. K. Freericks

Georgetown University

Collaborators: Tom Devereaux, Yizhi Ge, H. R.  
Krishnamurthy, Amy Liu, Brian Moritz, Thomas  
Pruschke

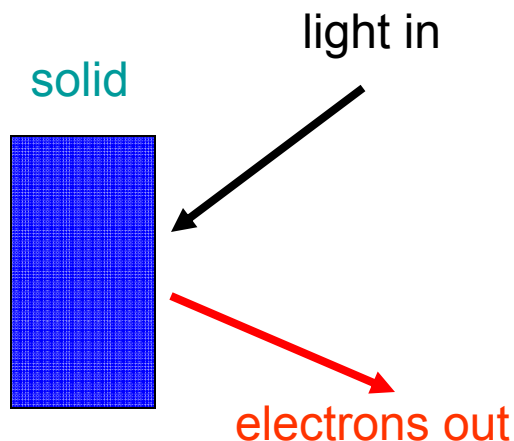
Funding: National Science Foundation

# Introduction

# Photoelectric effect



Einstein used the “old theory” of quantum mechanics to explain the photoelectric effect: Light carries discrete packets of energy related to its color. If a photon strikes an electron and has enough energy to knock the electron out of the material, then the electron is released and can be detected.

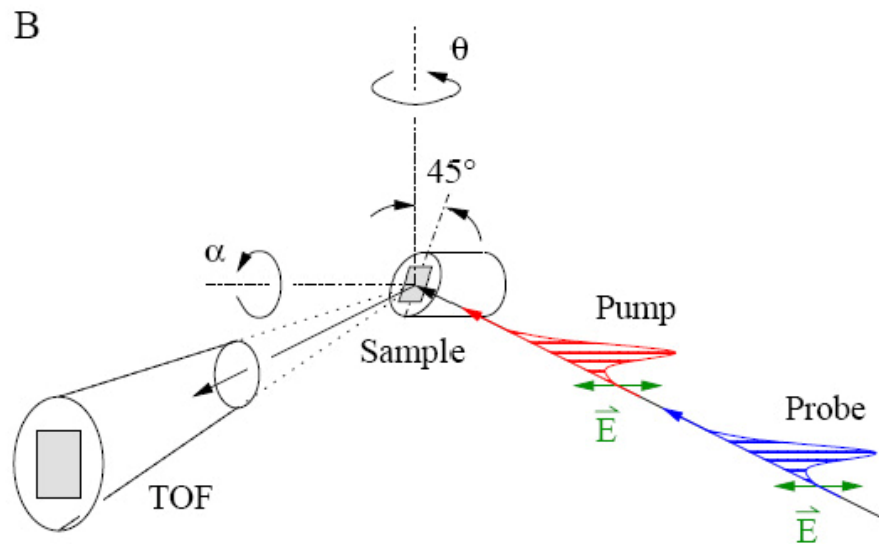


# Modern angle resolved photoelectron spectroscopy

Current experiments measure the angle and the energy of the emitted electron and can determine much about the equilibrium nature of the strongly correlated material: e. g. the high temperature superconductors.

But continuous beam ARPES only measures information about the occupied states in equilibrium.

# Time-resolved pump/probe photoelectron spectroscopy



Schematic of a TR-PES experiment  
(from Z.-X. Shen's group)

In a pump/probe experiment, we pump the system into an excited nonequilibrium state with an intense pulse of light.

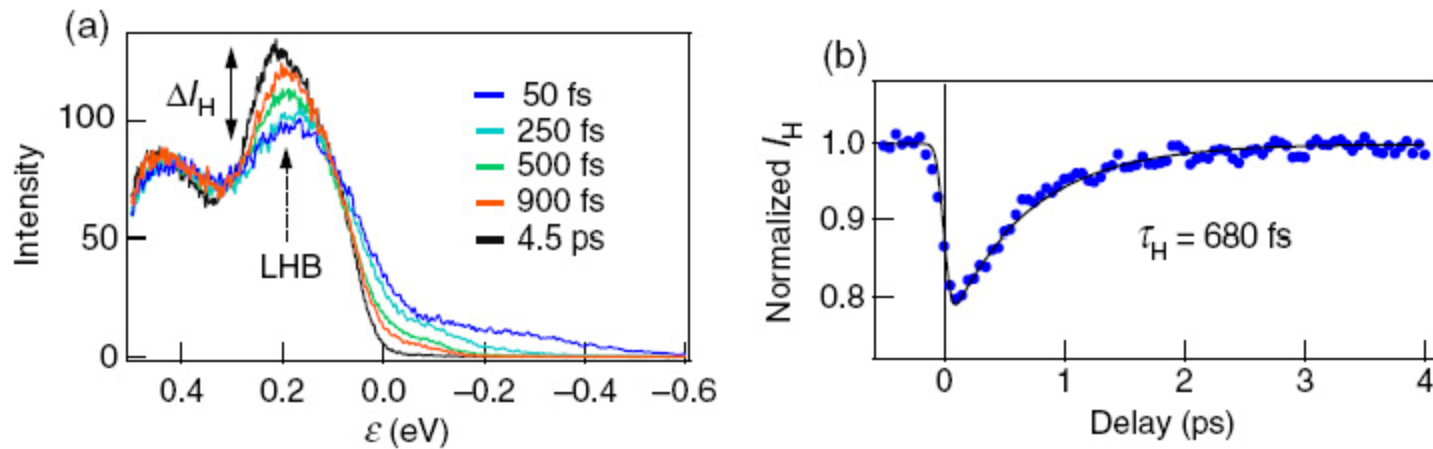
The system is then probed with a short pulse of light that is small amplitude but energetic enough to photo-emit electrons.

# Time-resolved pump/probe photoelectron spectroscopy

By varying the time delay between the pump and the probe, one can examine how the system relaxes from the nonequilibrium state generated by the pump to an equilibrium state after full relaxation.

This allows us to directly measure properties of nonequilibrium strongly correlated materials, a new frontier in condensed matter physics!

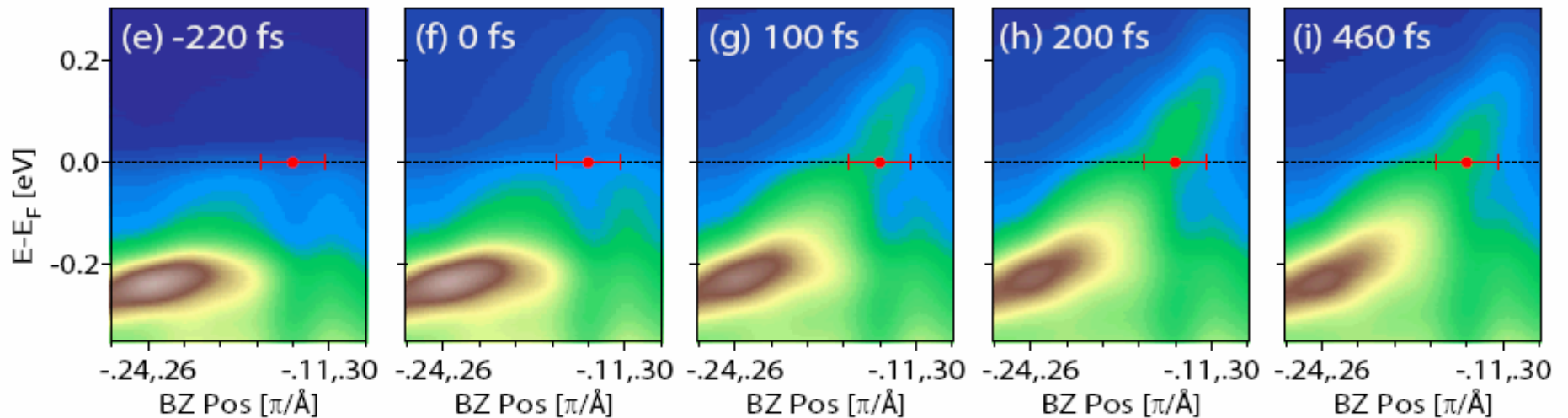
# TR-PES on TaS<sub>2</sub>



Experimental results by Perfetti et al. New Journal of Physics (2008)

One can clearly see that for short time delays the signal has much more high-energy spectral weight, which then relaxes to equilibrium at long times.

# TR-PES on $\text{TbTe}_3$



Experimental results by Schmitt et al. Science Express (2008)

Here one sees excitations above the Fermi energy at specific locations in the Brillouin zone.



# Theoretical formalism for TR-PES

# Nonequilibrium many-body physics

Since pumped systems do not have time-translation invariance, we must describe them with two-time Green's functions in the Kadanoff-Baym-Keldysh formalism.

Solving such problems is often much more complicated than equilibrium problems, but the solutions are much richer.

# TR-PES formalism

Our theory is developed in a scattering state approach with the sudden approximation. (More exact developments are also possible, but won't be described here.)

The system starts in equilibrium, is driven to nonequilibrium by the pump, and then relaxes back to equilibrium, being probed at different times after the pump is turned off.

# Keldysh boundary condition

In equilibrium, we have a set of initial states of the equilibrium Hamiltonian  $H$ , which satisfy  $H|\Psi_n\rangle = E_n|\Psi_n\rangle$ ,  $Z = \sum_n \exp(-\beta E_n)$ , and  $\rho_n = \exp(-\beta E_n)/Z$ .

Adding the pump changes  $H \rightarrow H_{\text{pump}}(t)$  and the unitary time evolution operator becomes

$$U(t_1, t_2) = T_t \exp[-i \int_{t_1}^{t_2} dt' H_{\text{pump}}(t')]$$

So evolving the equilibrium states under the pump corresponds to having an initial set of states  $\{|\Psi_n(t_0)\rangle\} = \{U(t_0, -\infty)|\Psi_n\rangle\}$  at time  $t_0$  when the probe is turned on (with the same Boltzmann weight  $\rho_n$ ).

$H_{\text{pump}}(t)$  is found by the Peierls' substitution:  
 $\varepsilon(\mathbf{k}) \rightarrow \varepsilon(\mathbf{k} - e\mathbf{a}A(t)/\hbar c)$ .

# Sudden approximation

The probe Hamiltonian is added at time  $t_0$ :

$H_{\text{pump}}(t) \rightarrow H_{\text{pump}}(t) + H_{\text{probe}}(t)$ , and our “final” set of states is  $\{|\Psi_n^F(t)\rangle\} = \{\hat{U}(t, t_0)|\Psi_n^I(t_0)\rangle\}$ , with the unitary evolution operator  $\hat{U}$  evolving with respect to the full Hamiltonian (pump plus probe).

The probability to detect a photoelectron with momentum  $\mathbf{k}_e = k_e \hat{e}_k$ , in range  $dk_e$  and solid angle  $d\Omega_{\hat{e}_k}$  is  $\lim_{t \rightarrow \infty} k_e^2 dk_e d\Omega_{\hat{e}_k} / (2\pi)^3 P(t)$  with  $P(t) = \sum_{mn} \rho_n |\langle \Psi_m; \mathbf{k}_e | \Psi_n^F(t) \rangle|^2$  and  $\langle \Psi_m; \mathbf{k}_e | = \langle \Psi_m | \otimes \langle \mathbf{k}_e |$  the direct product of a many-body state of the material and a scattering state with momentum  $\mathbf{k}_e$ , when far from the sample.

# Probe Hamiltonian

The probe Hamiltonian is

$$H_{\text{probe}}(t) = \int dk_z M(\mathbf{q}, \mathbf{k}, k_{ez}) s(t) a_{\mathbf{q}} c_{\mathbf{k}_e}^\dagger c_{\mathbf{k}}$$

where  $M$  is the matrix element and depends on the details of the modeling,  $s(t)$  is the envelope function of the probe pulse,  $a_{\mathbf{q}}$  annihilates a photon with momentum  $\mathbf{q}$ ,  $c_{\mathbf{k}_e}^\dagger$  creates a photoelectron with momentum  $\mathbf{k}_e$ , and  $c_{\mathbf{k}}$  removes an electron with momentum  $\mathbf{k}$ .

Since the probe pulse has a low amplitude, it is treated in lowest order perturbation theory, which shows that the excitation energy after the photoelectron has left is  $\omega = \omega_{\mathbf{q}} - W - k_e^2/2m$  and the matrix element satisfies

$$|\langle \Psi_m; \mathbf{k}_e | \Psi_n^F(t) \rangle| = \left| \int dk_z M(\mathbf{q}, \mathbf{k}, k_{ez}) \int_{t_0}^t dt' s(t') \exp[-i\omega(t-t_0)] \right. \\ \left. \times \langle \Psi_m | U^\dagger(t', t_0) c_{\mathbf{k}} U(t', t_0) | \Psi_n^I(t_0) \rangle \right|$$

# Final formula

The probability for detecting a photoelectron is then

$$P(t) = \int dk_z' \int dk_z M(\mathbf{q}, \mathbf{k}, k_{ez}) M^*(\mathbf{q}, \mathbf{k}', k_{ez}) I(t, \omega, \hat{\mathbf{e}}_{ke}; k_z, k_z')$$

with  $\mathbf{k} = (k_{||}, k_z)$ ,  $\mathbf{k}' = (k_{||}, k_z')$ , and

$$I(t, \omega, \hat{\mathbf{e}}_{ke}; k_z, k_z') = -i \int_{t_0}^t dt'' \int_{t_0}^t dt' s(t'') s(t') \exp[i\omega(t-t_0)] \\ \times G_{\mathbf{k}, \mathbf{k}'}^<(t', t'')$$

and the lesser Green's function is

$$G_{\mathbf{k}, \mathbf{k}'}^<(t', t'') = i \text{Tr} \{ \exp[-\beta H] c_{\mathbf{k}'}^\dagger(t') c_{\mathbf{k}}(t) \} / Z$$

with the operators in the Heisenberg picture with respect to  $H_{\text{pump}}(t)$ .

# Equilibrium continuous beam PES

In equilibrium, we have

$$G^<_{\mathbf{k},\mathbf{k}'}(t',t'')=G^<_{\mathbf{k},\mathbf{k}'}(t'-t'')$$

For a continuous beam experiment  $s(t)=1$ , and for a planar system we can neglect  $k_z$ , so the photoelectron transition rate becomes

$$\lim_{t \rightarrow \infty} \lim_{t' \rightarrow -\infty} I(t, \omega, \hat{\mathbf{e}}_{ke}) / (t-t_0) = -iG^<_{\mathbf{k}||}(\omega) = A_{\mathbf{k}||}(\omega) f(\omega)$$

which is the well-known result (when the matrix element is taken to be a constant).



# Quasiequilibrium pump/probe PES

In quasiequilibrium, we have

$$G^<_{\mathbf{k},\mathbf{k}'}(t',t'')=G^<_{\mathbf{k},\mathbf{k}'}(t'-t'')|_{T=T(\text{ave. time})}$$

but  $s(t) \neq 1$ , so

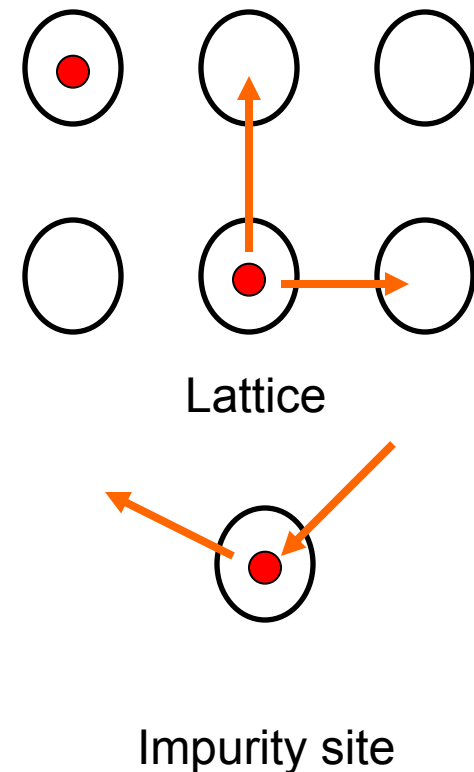
$$\lim_{t \rightarrow \infty} \lim_{t' \rightarrow -\infty} I(t, \omega, \hat{e}_{\mathbf{k}_e}) = -i \int d\omega' G^<_{\mathbf{k}_{||}}(\omega - \omega') |\hat{s}(\omega')|^2$$

with  $\hat{s}(\omega')$  the Fourier transform of  $s(t)$ . This implies there can be a “windowing effect” on the TR-PES signal even in the quasiequilibrium approximation. For  $\text{TaS}_2$ , this is not important because the width of the Fourier transform of the probe envelope is 8 meV, and the features in the DOS are on the 30-100meV range.

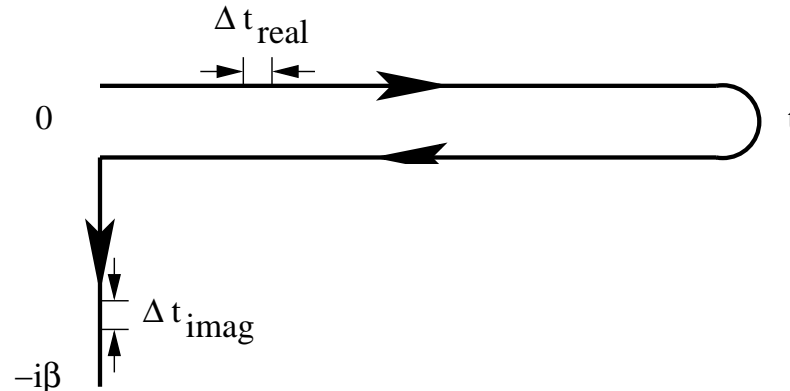
# Calculating the transient nonequilibrium response

# Dynamical mean field theory

- Models of strongly correlated electrons are difficult to solve.
- Significant progress has been made over the past 19 years by examining the limit of **large spatial dimensions**.
- In this case, the lattice problem can be mapped onto a self-consistent impurity (single-site) problem, in a time-dependent field that **mimics the hopping of electrons onto and off of the lattice sites**.



# Kadanoff-Baym-Keldysh formalism



- Problems without time-translation invariance can be solved with a so-called **Keldysh formalism**.
- Green's functions are defined with time arguments that run over the **Kadanoff-Baym-Keldysh contour**.
- The electrons evolve in the fields **forwards** in time, then de-evolve in the fields **backwards** in time.

# DMFT algorithm

**Dyson equation**

$$\Sigma = G_0^{-1} - G_{\text{loc}}^{-1}$$

**Hilbert transform**

$$G_{\text{loc}} = \sum_k [G_k^{\text{non-1}}(E) - \Sigma]^{-1}$$

**Dyson equation**

$$G_0 = (G_{\text{loc}}^{-1} + \Sigma)^{-1}$$

$$G_{\text{loc}} = \text{Functional}(G_0)$$

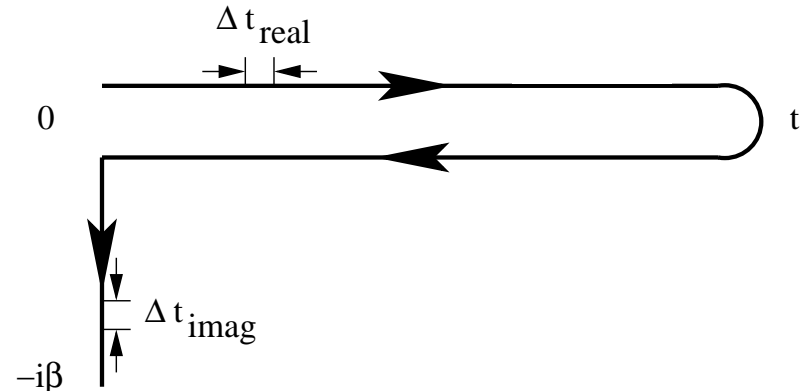
{example: FK model:

$$G_{\text{loc}} = (1 - w_1)G_0(\mu) + w_1 G_0(\mu - U)}$$

**Solve impurity  
problem**

All objects ( $G$  and  $\Sigma$ ) are **matrices** with each time argument lying on the contour.

# Computational elements



The key issue in calculating the real-time Green's function is to evaluate the **Dyson equation of a continuous integral operator** defined on the Kadanoff-Baym-Keldysh contour.

This operator is first **discretized** on a grid to be represented by **finite-dimensional** matrices.

Next, we need to integrate the dependence of the **matrix elements** over a **two-dimensional** energy space.

Each matrix element is constructed from **one matrix inverse** and **two matrix multiplications**. We typically work with (approximately 10,000) **general complex matrices** of size up to 5700X5700.

Since the only information needed to generate the matrices is the local self-energy matrix  $\Sigma$ , the electric field  $\mathbf{E}$ , and the temperature  $T$ , **this procedure is easily parallelized**.

# Quasiequilibrium approach

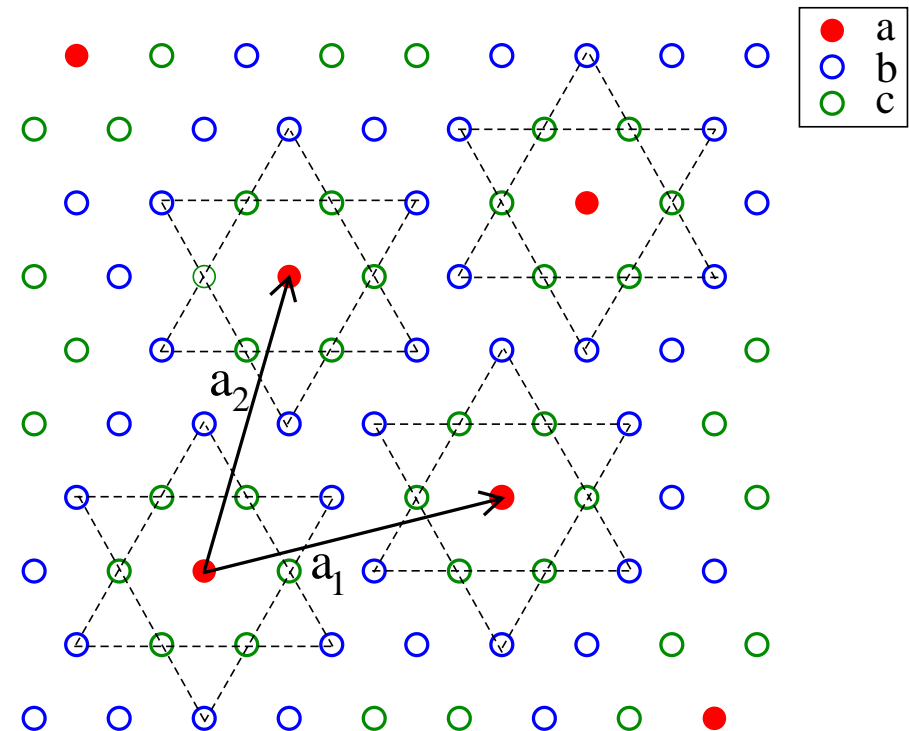
- Assume the temperature varies with the average time and use equilibrium solvers to solve for the response function.
- Here we examine the single-band Hubbard model with the numerical renormalization group (NRG) as the solver.
- This assumes the Hubbard bands do not overlap with any other bands in the system---an assumption that does not hold for  $\text{TaS}_2$ .

# Modeling TaS<sub>2</sub>

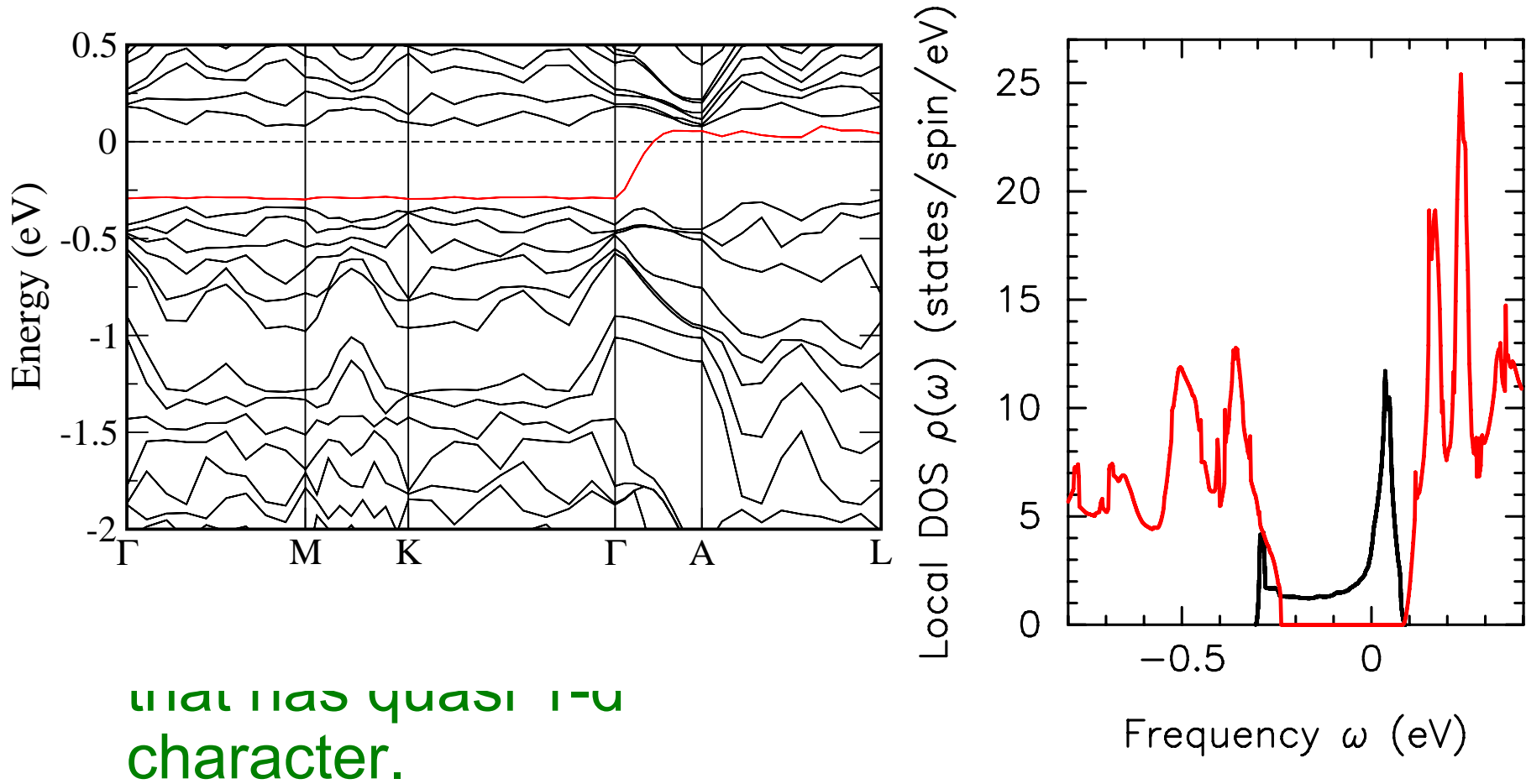


# CDW in

- At high T,  $\text{TaS}_2$  has triangular S-Ta-S planes.
- Below 180K, a commensurate CDW forms with a “Star of David” structure.



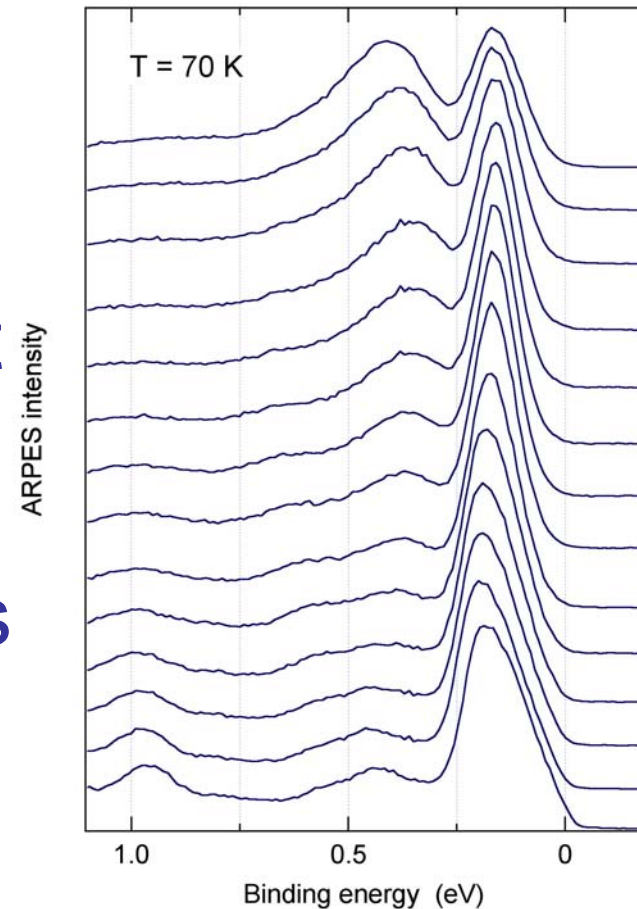
# CDW orbit coupling



that has quasi 1D  
character.

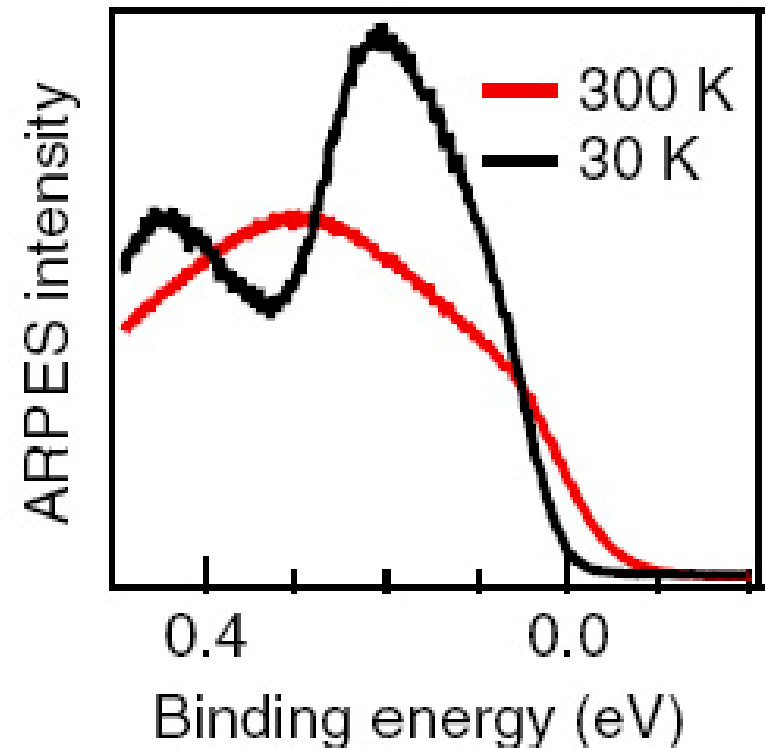
# Continuous beam equilibrium ARPES at 70K (Grioni's group)

- Note the limited dispersion of the main peak.
- Note also that it does not appear insulating, even though the bulk material has a 0.1-0.15 eV gap as seen in optical conductivity.



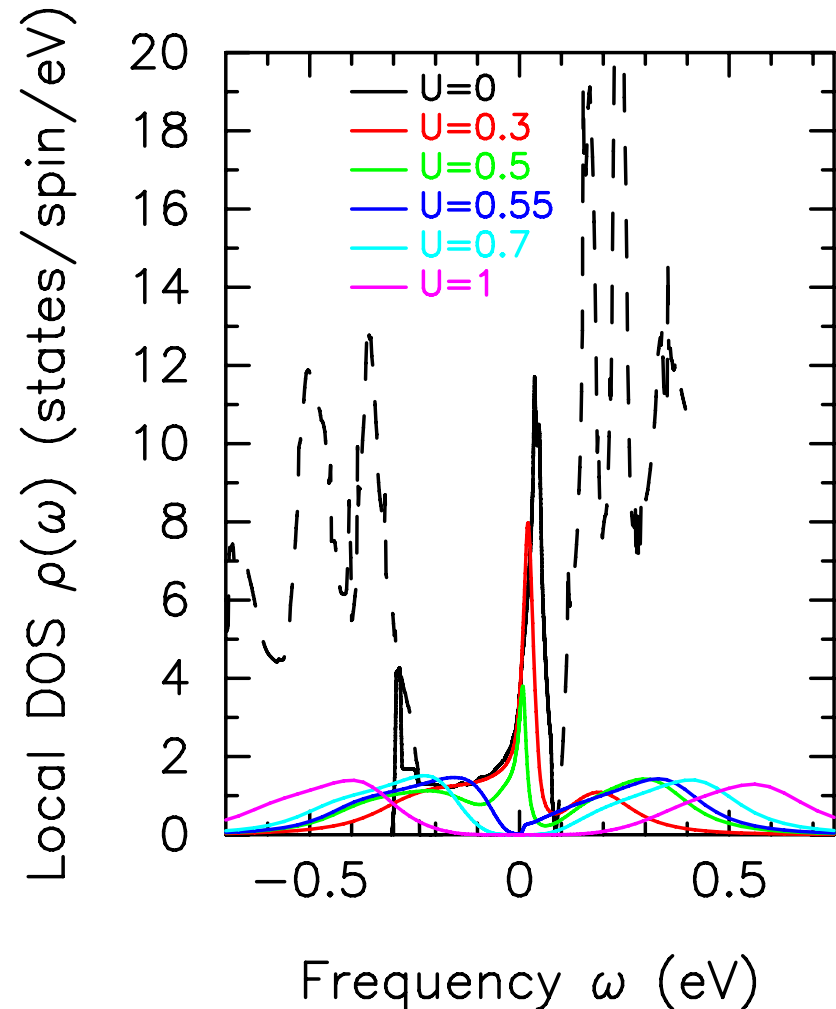
# Lower energy photon PES at 300K and 30K (Perfetti et al.)

- As  $T$  is lowered from an incommensurate CDW (metal) to a commensurate CDW (insulator), we see a low-energy band splitting off.
- This band is believed to be the lower Hubbard band of the correlated band that crosses the Fermi energy.

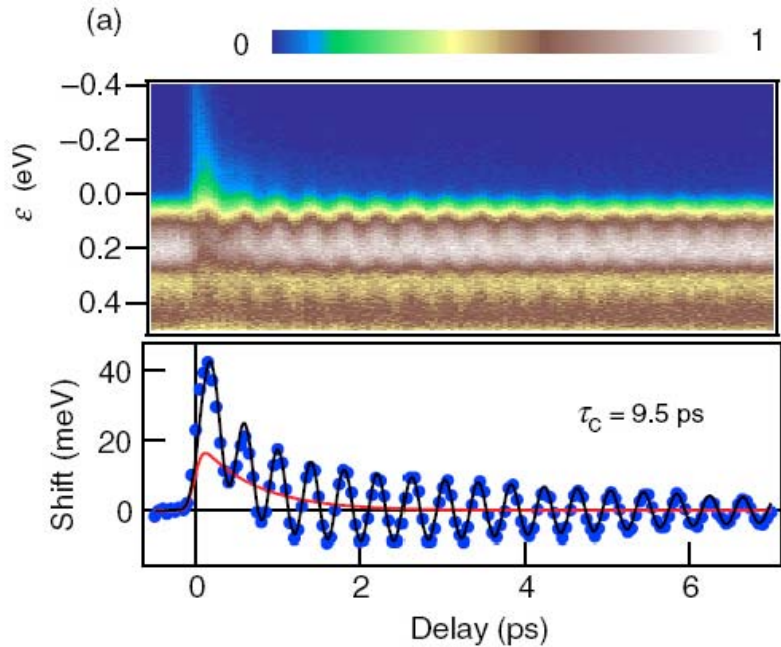


# Fitting the Hubbard U

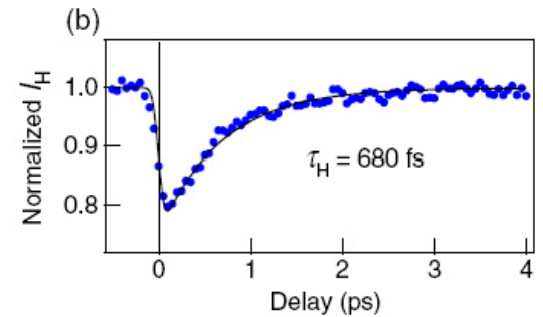
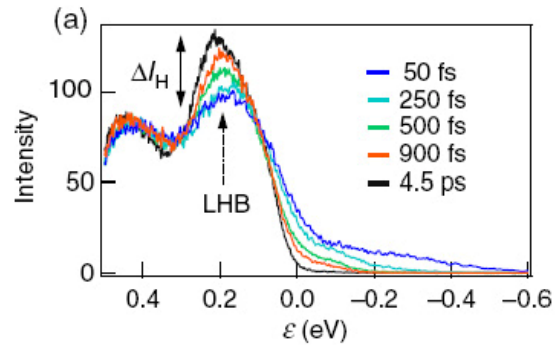
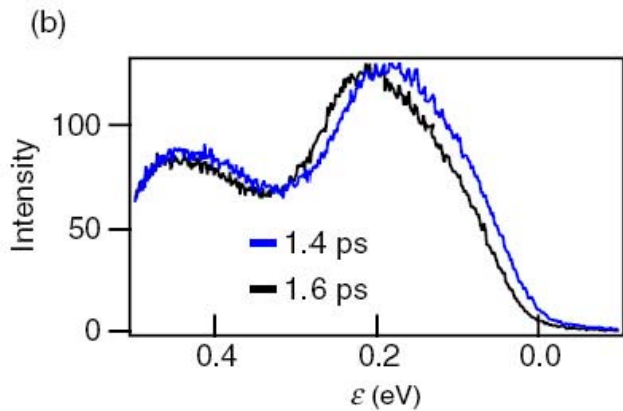
- As  $U$  increases we see the metallic behavior disappear and a gap form at  $U_c=0.55$ .
- An experimental gap of 0.15 eV requires  $U=0.7$  eV.



# Pump/Probe TR-PES

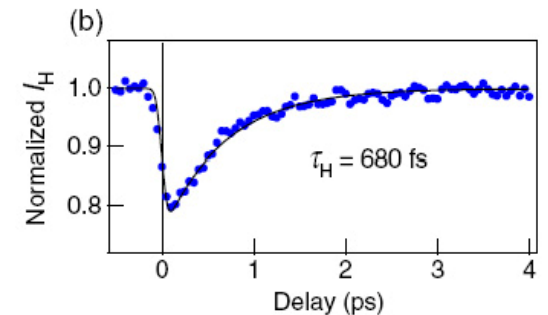
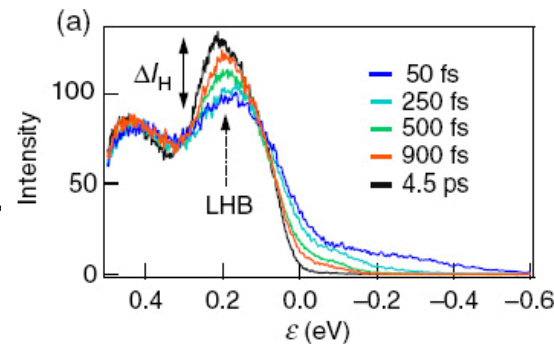
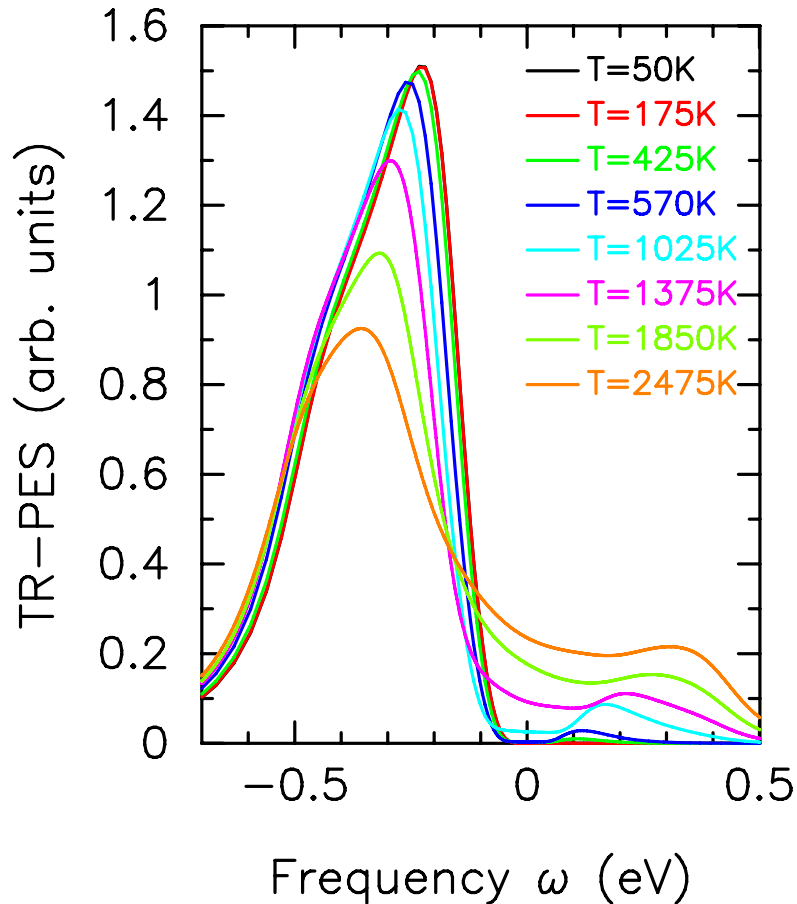


- The signal oscillates over a long period of time due to coupling of the electronic degrees of freedom with the optical phonons.
- At short times, one can see higher energy states occupied, and then they relax back to equilibrium.

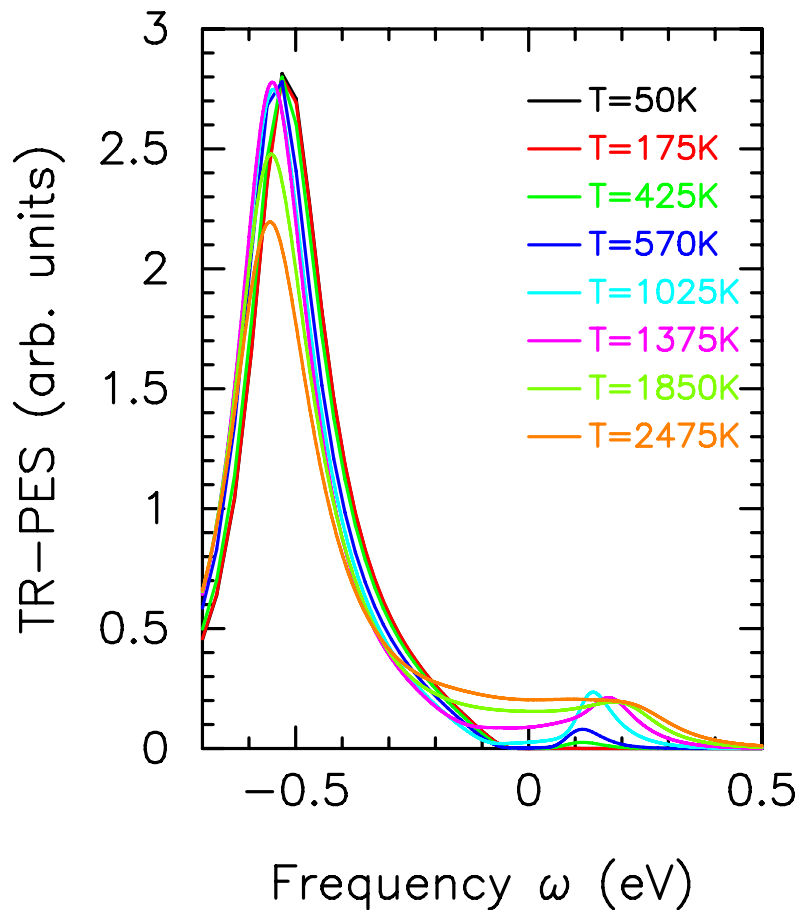


# Local GF TR-PES

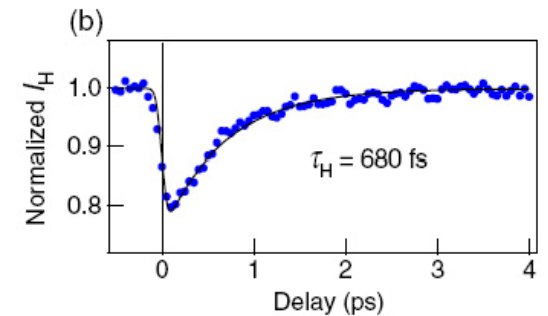
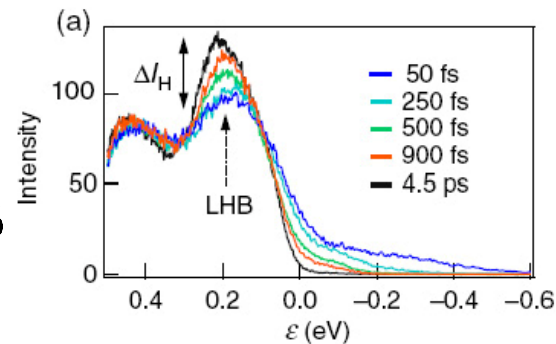
- The theoretical prediction shows a leftward movement of the peak, clearly shows the insulator and the upper Hubbard band.
- In experiment, the peak moves to the right, the gap is never seen, and the upper Hubbard peak is not seen.



# K=0 GF TR-PES

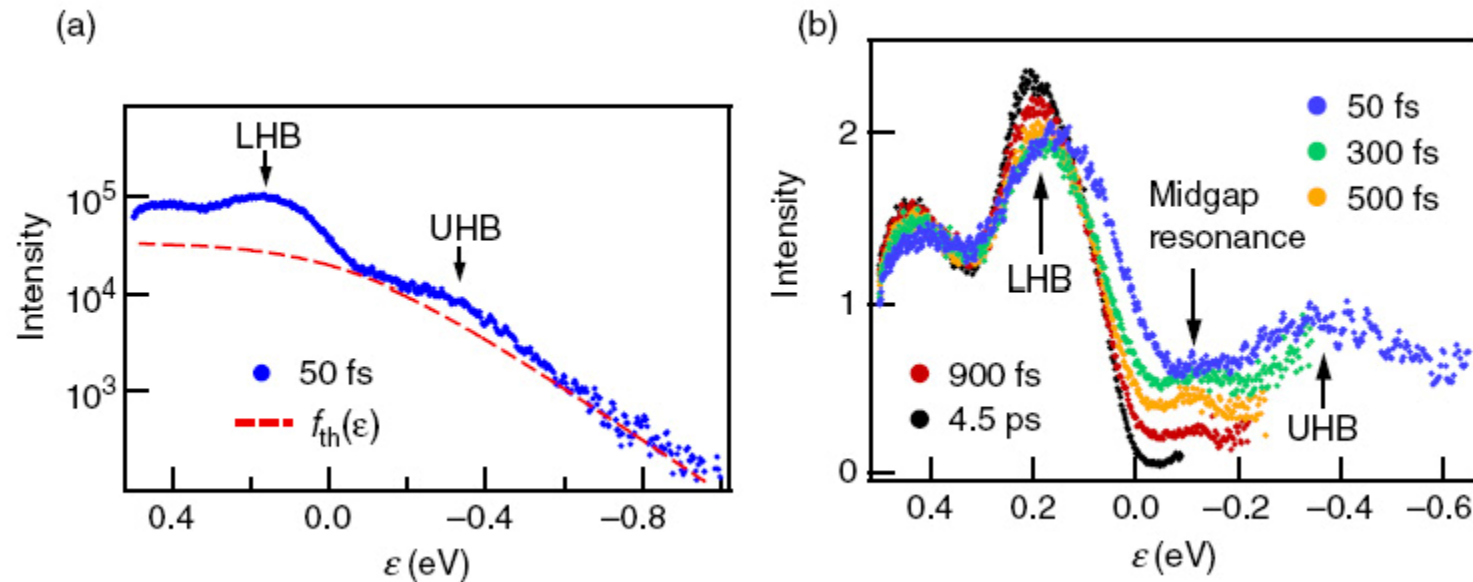


- Here the curvature might be closer to experiment, and the sharp upper Hubbard band feature is reduced.
- But it still does not agree with experiment.





# Experimental DOS by division with a Fermi factor



- In experiment, they try to extract the DOS by dividing out the Fermi factor which has an effective temperature fit to the data.
- They see a midgap resonance when they do this.

# Discussion

# Theoretical issues

- We use DMFT for a quasi one-dimensional system.
- Averaging over  $k_z$  should be done rather than using a  $k=0$  spectral function.
- Overlap of upper Hubbard band with other (noninteracting) bands means the nonequilibrium modeling of the occupation of the Hubbard band is incorrect.
- Theory sees an insulator but no midgap resonance.

# Conclusions/Future Work

- Using DMFT for a quasi one-d system may be OK in the Mott phase, where most of the physics is local.
- Overlap of the upper Hubbard band with noninteracting bands can be treated simply by assuming those bands act like an electron reservoir and remove electrons from the Hubbard band; this could then give rise to a midgap resonance of the Fermi liquid.
- Suppression of the insulating gap may occur due to surface states and matrix-element effects not taken into account here.